Available online at www.sciencedirect.com
SCIENCE DIRECT®
PERGAMON
International Journal of Heat and Mass Transfer 46 (2003) 2833–2839
International Journal of HEAT and MASS TRANSFER
www.elsevier.com/locate/ijhmt

Shape optimization of cut-off in a multi-blade fan/scroll system using neural network

S.-Y. Han *, J.-S. Maeng

School of Mechanical Engineering, Hanyang University, 17 Haengdang-Dong, Sungdong-Gu, Seoul 133-791, South Korea

Received 1 April 2002; received in revised form 6 January 2003

Abstract

In order to improve efficiency of a system with three-dimensional flow characteristics, this paper presents a new method that overcomes the computational difficulties associated with three-dimensional effects by using two-dimensional CFD and a neural network. The method was applied to the shape optimization of cut-off in a multi-blade fan/scroll system. As for the entrance conditions of two-dimensional CFD analysis, the experimental values at the positions apart from the inactive zone were used. The distributions of velocity and pressure obtained by two-dimensional CFD analysis were compared with those of three-dimensional CFD analysis and experimental results. It was found that the distributions of velocity and pressure have qualitative similarity. The results of two-dimensional CFD analysis were used for learning as target values of a neural network. The optimal angle and radius of cut-off were determined as 71° and 0.092 times the outer diameter of impeller, respectively. It was concretized in a previous report that the optimal angle and radius of cut-off are approximately 72° and 0.08 times the outer diameter of impeller, respectively.

Keywords: Multi-blade fan/scroll system; Cut-off; Inactive zone; Neural network; Optimization

1. Introduction

A multi-blade fan/scroll system is the core part of an air conditioning system. The flow field of the multi-blade fan/scroll system becomes very complicated because of the characteristic geometrical shape. As fluid enters into the axial direction of a rotor and goes on to scroll through the radial direction of an impeller, an inactive zone is generated at the entrance of the impeller and its size is not uniform in both the axial and circumferential directions [1,2].

The inactive zone indicates the region where smooth flowing is not formed at the entrance of the impeller because of the rotation of fluid. It causes a decrease of flow efficiency and sometimes generates a noise of fluid flow as well as that of vibration.

Most studies on the improvement of efficiency particularly focused on a cut-off among various design variables such as the twisting angle, shape and number of a blade, the shape of fan and scroll, or the clearance between fan and cut-off. Raj [3] reported that the best efficiency could be obtained at around the angle of 72°, and Morinushi [4] insisted that the radius of cut-off would be near 0.08 times the outer diameter of an impeller for the best efficiency. Humbad [5] verified that the separation occurring on cut-off is a major cause of noise. And Maeng [6] studied the characteristics of the inactive zone and considered the change of volume flow rate due to various curvature radii of the cut-off experimentally.

The purpose of this study was to increase the flow efficiency of a multi-blade fan/scroll system, so it was intended to obtain an optimal angle and curvature radius of the cut-off systematically. Instead of three-dimensional CFD analyses, two-dimensional calculations were

* Corresponding author.
E-mail addresses: syhan@email.hanyang.ac.kr (S.-Y. Han), jsmaeng@hanyang.ac.kr (J.-S. Maeng).

0017-9310/03/$ - see front matter
doi:10.1016/S0017-9310(03)00066-8

Nomenclature

A	learned value	$r_{\text{cut-off}}$	curvature radius of cut-off
b	width of an impeller	r_s	shape function of a scroll
C_1	cord length of a blade	T	target value for neural network
D_1	inner diameter of an impeller	t	distance between bell mouth and impeller
D_2	outer diameter of an impeller	$\overline{u_i u_j}$	Reynolds stress
I_z	size of inactive zone	V_i	turbulent mean velocity
L	width of a scroll	k	turbulent kinetic energy
n	revolution per minute of a fan [rpm]	ε	energy dissipation
p	pressure	θ	coordinate of the circumferential direction of impeller
r	coordinate of the radial direction of an impeller	$\theta_{\text{cut-off}}$	angle of cut-off from the base line [°]
r_1	inner radius of an impeller	μ	coefficient of viscosity
r_2	outer radius of an impeller	ψ	coefficient of pressure
r_c	clearance between fan and cut-off (clearance of cut-off)		

performed. In order to get input data for the two-dimensional CFD calculations, experiments were carried out for the various angles and curvatures of cut-off. The validity of the two-dimensional CFD analysis was examined by comparing separation phenomenon qualitatively with the three-dimensional calculations. In order to examine the validity that the result of the two-dimensional CFD analysis is in good agreement with the three-dimensional phenomenon, the result was compared with the previous studies [7,8]. Then the neural network was applied for optimal angle and curvature radius of cut-off, where the separation phenomenon becomes the minimum. As target values for learning a neural network, the numerical results of two-dimensional CFD analyses were used. Then the optimal angle and radius of cut-off were quantitatively determined from the learned neural network. Therefore, it was concretized the previous reports [3,4] that the optimal angle and radius of cut-off are approximately 72° and 0.08 times the outer diameter of the impeller, respectively.

2. Flow analysis

2.1. Geometrical shape

The geometrical shape used in this study is shown in Fig. 1. The external curve of the scroll is an exponential function of $r = 179e^{0.114\theta}$. The fan specification of the angles and curvatures of cut-off for five cases and seven cases, respectively, are tabulated in Table 1.

2.2. Numerical analysis

The governing equations of two-dimensional incompressible steady flow are as follows:

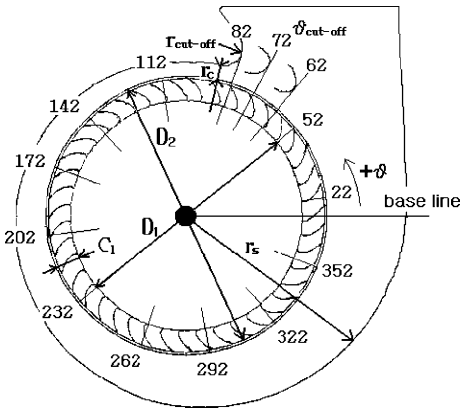

Fig. 1. Fan configuration.

Table 1
Fan specification

Designation	Size
D_2 (mm)	326
D_1 (mm)	271
C_1 (mm)	55
b (mm)	65
Z (no. of blades)	50
n (rpm)	700
$r_{\text{cut-off}}$	$0.06D_2$–$0.12D_2$
$\theta_{\text{cut-off}}$	62°, 67°, 72°, 77°, 82°
t	$0.12b$

- Continuity equation

$$\frac{\partial V_i}{\partial x_i} = 0 \tag{1}$$

- Reynolds averaged momentum equation

$$\frac{DV_i}{Dt} = \frac{1}{\rho}\frac{\partial p}{\partial x_i} + v\frac{\partial^2 V_i}{\partial x_j \partial x_j} - \frac{\partial}{\partial x_j}\overline{u_i u_j} \tag{2}$$

- Standard k–ε model

$$\frac{Dk}{Dt} = \frac{\partial}{\partial x_j}\left[\left(C_k\frac{k^2}{\varepsilon} + v\right)\frac{\partial k}{\partial x_i}\right] - \overline{u_i u_j}\frac{\partial V_i}{\partial x_j} \tag{3}$$

$$\frac{D\varepsilon}{Dt} = \frac{\partial}{\partial x_j}\left[\left(C_\varepsilon\frac{k^2}{\varepsilon} + v\right)\frac{\partial \varepsilon}{\partial x_j}\right] - C_{\varepsilon_1}\frac{\varepsilon}{k}\overline{u_i u_j}\frac{\partial V_i}{\partial x_j} - C_{\varepsilon_2}\frac{\varepsilon^2}{k} \tag{4}$$

Multi-block approach was applied to computational mesh for flow analysis because of the complicated shape. The flow field was divided into 53 regions, and a 30,000–33,000 structured grid was generated for each model, as shown in Fig. 2. The governing equations were solved by the finite volume method with SIMPLEC algorithm. The second order upwind scheme was applied to the convection term, the first order upwind scheme was applied to the turbulence equation, and standard k–ε model was applied to the turbulence model.

2.3. Boundary conditions

Boundary conditions at the entrance of the impeller for two-dimensional CFD analysis were obtained from the results of experiments for the specified models tabulated in Table 1. Fig. 3 shows the distribution and size of the inactive zone in the circumferential direction, which were measured by 5-hole pitot tubes and by photo analyses of the flow visualization method using smoke, as shown in Fig. 4. I_z is a dimensionless value of the inactive zone normalized by the width b of the impeller [6].

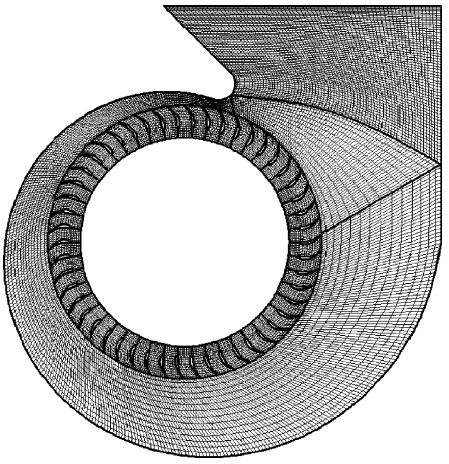

Fig. 2. Computational mesh.

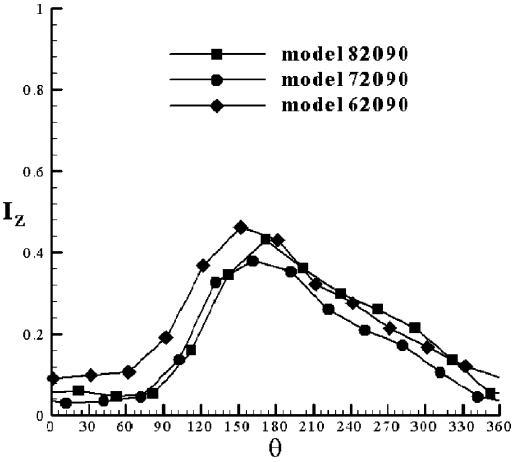

Fig. 3. Size of inactive zone.

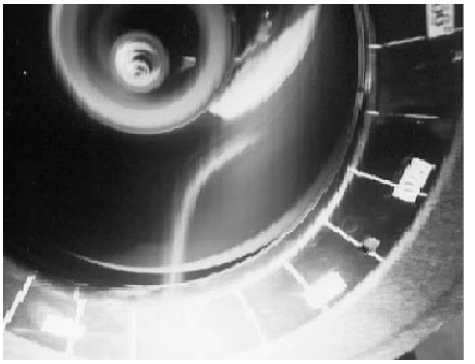

Fig. 4. Flow visualization using smoke.

It was found that the maximum inactive zones are formulated at the angles of the cut-off between 150° and 180° from Fig. 3. Also, the inactive zones influence around the 50% location of the impeller's width from the entrance of the fan. Therefore, as input data for two-dimensional CFD analysis, the experimental values distributed in the circumferential direction at the 60% location of the impeller's width from the entrance of the fan, where flow field is not influenced by the inactive zones were used. A constant pressure condition was used for the exit and a rotating wall boundary condition was used for multi-blade rows.

In Fig. 3, the notation of model 82090 indicates that the angle [°] of cut-off is 82° is, whereas its radius is 0.09 times the outer diameter of the impeller.

2.4. Result of numerical analysis

In order to examine whether the result of the two-dimensional CFD analysis can be applied to a three-dimensional multi-blade fan/scroll system qualitatively,

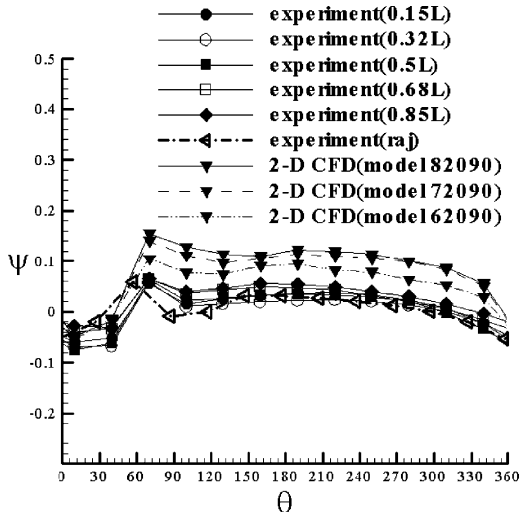

Fig. 5. Comparison of pressure coefficient at $1.13D_2$.

pressure coefficients of experimental measurement values and two-dimensional CFD analyses were qualitatively compared for various sections in the shaft direction. Also, pressure distributions of the three-dimensional and two-dimensional CFD analyses were qualitatively compared.

Fig. 5 shows the comparison of the pressure coefficient distribution of each model in the circumferential direction at the 1.13D2 in the radial direction from the fan center. In the figure, the pressure coefficients of the two-dimensional CFD analyses were compared with those of Raj [3] and experiments conducted in this study. The pressure distributions were measured for five sections (0.15, 0.32, 0.5, 0.68, 0.85 L from the entrance of a fan) in the shaft direction by 5-hole pitot tube. It was found that the pressure coefficient distributions are qualitatively very similar to one another.

Fig. 6 shows the velocity vectors and pressure field of model 72090 obtained by the three-dimensional CFD analysis. Comparing them with those of the two-dimensional CFD analysis for the same model as shown in Fig. 7, the minimum pressures are found around the exit of the impeller and cut-off between the angles of the cut-off, 0° and 60°. Also, both the velocity vectors in the radial and the circumferential direction show a very similar profile although the quantitative magnitudes of the velocities are different. This can be verified from the experimental results of Refs. [7] and [8]. Volume flow rates were calculated by the average velocity times the area at the exit, and tabulated in Table 2. Fig. 8 shows the comparison of volume flow rates for nine models between experimental measurement and the two-dimensional CFD analysis. It was found that the changes of the volume flow rates coincide with each model qualitatively.

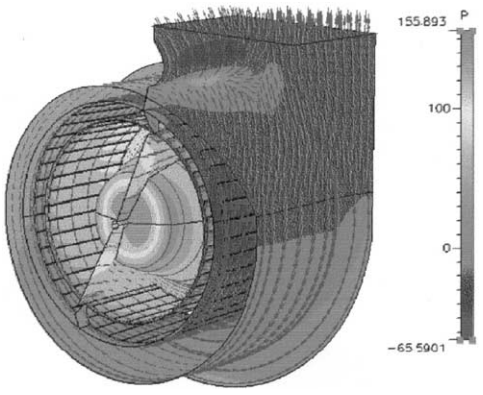

Fig. 6. Velocity vector and pressure contour (3D-CFD).

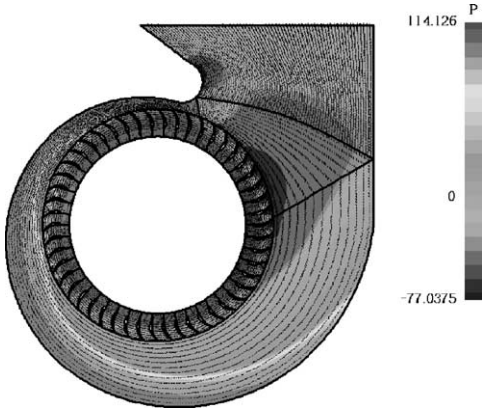

Fig. 7. Velocity vector and pressure contour (2D-CFD).

Therefore, it was confirmed that there is kinematic similarity between the results of the two-dimensional and three-dimensional CFD analyses, and so, the result of the two-dimensional CFD analysis can be applied to the three-dimensional multi-blade fan/scroll system qualitatively.

3. Optimal angle and radius of cut-off

3.1. Constitution of neural network

The volume flow rates obtained by the two-dimensional CFD analysis were used as target values for learning a neural network [9]. The angle and radius of the cut-off were established as design variables, and the ranges of the angle and radius were 67–77° and $0.06D_2$–$0.12D_2$, respectively. A neural network was constituted based on MATLAB. The neural network was constituted of one input layer, one output layer and two hidden layers, as shown Fig. 9. The numbers of neuron

Table 2
Volume flow rate analysis using CFD (m^3/min)

$r_{cut\text{-}off}$	$\theta_{cut\text{-}off}$				
	62°	67°	72°	77°	82°
$0.06D_2$	28.184	28.433	28.936	28.768	28.714
$0.07D_2$	28.401	28.737	29.406	29.070	28.802
$0.08D_2$	28.448	29.031	29.833	29.334	28.863
$0.09D_2$	28.475	29.333	30.040	29.627	28.977
$0.10D_2$	28.426	29.074	30.011	29.333	28.836
$0.11D_2$	28.285	28.958	29.764	29.045	28.373
$0.12D_2$	28.129	28.581	29.519	28.759	28.055

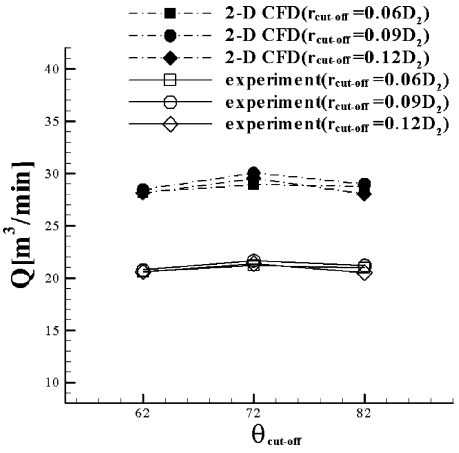

Fig. 8. Comparison of volume flow rate.

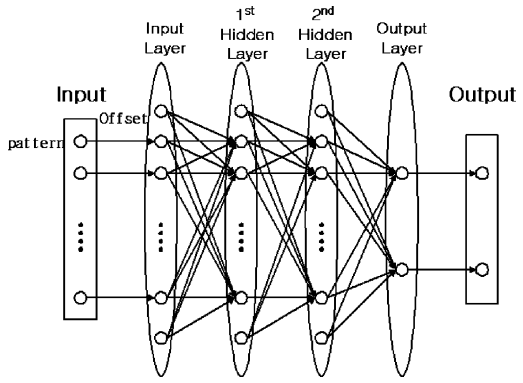

Fig. 9. Structure of neural network.

for two hidden layers were 60 and 30, respectively. Error backpropagation rule was applied as a learning method. Hyperbolic tangent sigmoid transfer function was used as a connection function between the input layer and the first hidden layer, and between the first hidden layer and the second hidden layer. Hard limit transfer function was used between the second hidden layer and the output layer. The error was allowed to 10–6 in order to obtain a more accurate solution.

3.2. The result of learning neural network

By learning the above neural network with the target values, the values of learning results shown in Table 3 were obtained, which almost coincide with the values of CFD listed in Table 2. The relation between the values of the learning result and those of CFD was obtained by Eq. (5). In Eq. (5), A indicates the output values of learning the neural network whereas T means the target values obtained from CFD analysis. The relation between the values is plotted in Fig. 10. It was found from

Table 3
Volume flow rate analysis using neural network (m^3/min)

$r_{cut\text{-}off}$	$\theta_{cut\text{-}off}$		
	67°	72°	77°
$0.06D_2$	28.433	28.937	28.768
$0.07D_2$	28.735	29.406	29.070
$0.08D_2$	29.032	29.833	29.335
$0.09D_2$	29.333	30.040	29.627
$0.10D_2$	29.071	30.013	29.333
$0.11D_2$	28.959	29.764	29.045
$0.12D_2$	28.581	29.520	28.759

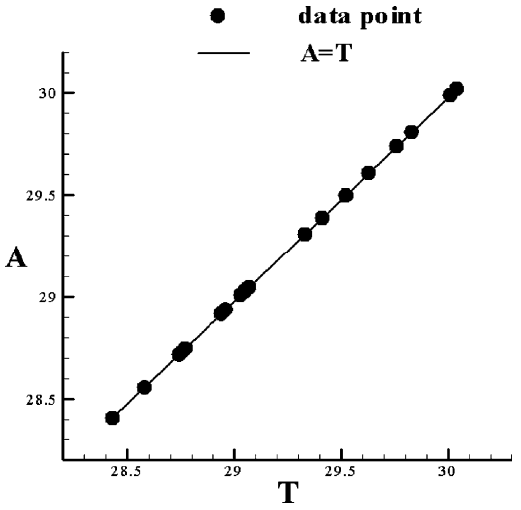

Fig. 10. Correlation between object value and learning result value.

Fig. 10 that the correlation between the values is very high.

$$A = T - 0.0206 \tag{5}$$

4. Results of neural network

The learning results of the neural network for the angles and radii of cut-off in three-dimensional space are shown in Fig. 11. From the figure, it is found that the high volume flow rates are shown in the ranges of angles 70–74°, and in the ranges of the radius $0.88D_2$–$0.102D_2$, respectively. The optimal values of the angle and the radius of cut-off were obtained by 71° and $0.092D_2$, respectively. For the optimal angle and radius of cut-off,

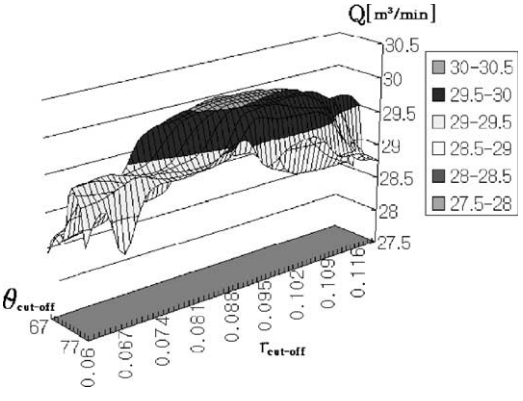

Fig. 11. Volume flow rate analysis (m^3/min).

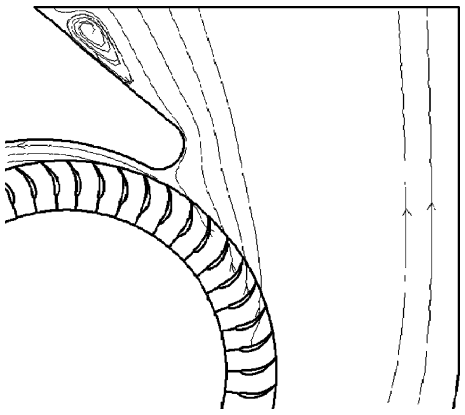

Fig. 12. Streamline distribution (model 62090).

the maximum volume flow rate was obtained as 30.055 m^3/min.

Streamline distributions of the flow field due to various angles and radii of cut-off are shown in Figs. 12–14. In Fig. 12, it was shown that a large separation occurred around the exit for the angle of cut-off, 62°. It was found that separation size was reduced a little bit as shown in Fig. 13 for the larger angle of cut-off, 67°, as compared with Fig. 12. And it was verified that separation almost diminished for the optimal angle of cut-off, 71°, as shown in Fig. 14. It can also be found from Fig. 3 that the less the size of separation is, the less the size of inactive zone is, too.

If the angle of cut-off is larger than the optimal angle, separation does not occur around the exit. However, since the inactive zone increased as shown in Fig. 3, flow efficiency becomes so low that the volume flow rate is reduced [6].

Therefore, the optimal angle and radius of cut-off agrees well with the measurement results of volume flow rate change due to the size of the inactive zone as shown

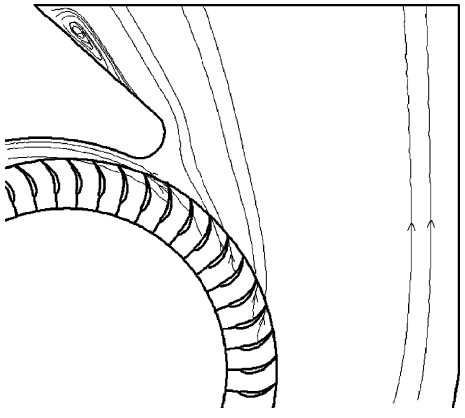

Fig. 13. Streamline distribution (model 67090).

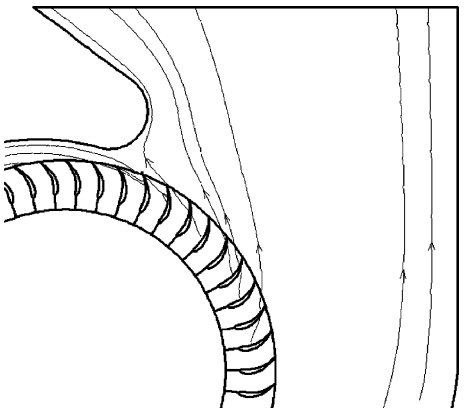

Fig. 14. Streamline distribution for optimized model.

in Fig. 8. The clearance between fan and cut-off, which highly influences flow efficiency, is easily determined as the optimal angle and radius of cut-off are determined, since it is a function of the angle and radius of cut-off.

5. Conclusions

In order to minimize the inactive zone of unstable flow occurring at a multi-blade fan/scroll system, the two-dimensional turbulent fluid field analyses and neural network technique were applied. From the results of computational fluid analyses and neural network technique, the following conclusions were obtained:

(1) The optimal angle and radius of cut-off were determined as 71° and 0.092 times the outer diameter of the impeller, respectively.
(2) From the result of two-dimensional turbulence flow field analysis for the optimal angle and radius of cut-off, it was verified that the maximum flow rate can be obtained by diminishing the separation zone around the cut-off.
(3) By combining the two-dimensional flow analysis and optimization technique for a complicated turbulence flow field such as a multi-blade fan/scroll system, the optimal angle, radius and clearance of cut-off can be determined.

References

[1] R.J. Kind, M.G. Tobin, Flow in a centrifugal fan of the squirrel cage type, Trans. JSME 52 (484) (1990) 3987–3991.
[2] J.S. Maeng, J.Y. Yoon, T.B. Ahn, J.E. Yoon, D.J. Han, An experimental study for flow characteristics inside the rotor of a multi-blade fan/scroll system, Trans. KSME Ser. B 23 (5) (1999) 646–652.
[3] D. Raj, W.B. Swim, Measurements of the mean flow velocity and velocity fluctuations at the exit of a FC centrifugal fan rotor, J. Eng. Power 103 (1981) 393–399.
[4] K. Morinushi, The influence of parameters on F.C. centrifugal fan noise, Trans. ASME, J. Vibration, Acoustics, Stress, Feliability Des. 109 (1987) 227–234.
[5] N.G. Humbad et al., Case study on reducing automotive blower rumble noise, in: Proceeding of the ASME Noise and control division, Nca-vol. 22, 1996, pp. 233–242.
[6] J.S. Maeng, D.H. Yoo, K.H. Lee, I.K. Park, Some relations between the geometric parameters and internal flow field characteristics in multiblade fan/scroll system, Trans. KSME Ser. B 24 (9) (2000) 1139–1147.
[7] G.R. Denger, M.W. Mcbride, G.C. Lauchle, An Experimental Evaluation of the Internal Flow Field of an Automotive Heating, Ventilating and Air Conditioning System, Technical Report No. TR 90-011, Pennsylvania State University, 1990.
[8] S. Yamazaki, R. Satoh, An experimental study on the aerodynamic performance of multiblade blowers, Trans. JSME 52 (484) (1986) 3987–3991.
[9] Y.D. Lim, S.B. Lee, Fuzzy Neural Network, Genetic Evolution, Young and Il, pp. 107–144.